Analysis and Benchmarking of Radial Flux Cycloidal Magnetic Gears with Reduced Permanent Magnet Piece Count Using Consequent Poles

Matthew Johnson
US Army Research Laboratory
US Army DEVCOM
College Station, TX, USA
matthew.c.johnson186.civ@mail.mil

Shima Hasanpour
Dept. of Elec. & Comp. Eng
Texas A&M University
College Station, TX, USA
shimahasanpour@tamu.edu

Matthew C. Gardner
Dept. of Elec. & Comp. Eng
University of Texas at Dallas
Richardson, TX, USA
matthew.gardner@utdallas.edu

Hamid A. Toliyat
Dept. of Elec. & Comp. Eng
Texas A&M University
College Station, TX, USA
toliyat@tamu.edu

***Abstract*—Magnetic gears employ magnetic fields, rather than teeth, to perform the gearing action. At large gear ratios, cycloidal magnetic gears (CyMGs) can achieve higher torque densities than the more common coaxial magnetic gears. This paper compares CyMG topologies with consequent pole (CP) rotors against CyMGs with more conventional surface permanent magnet (SPM) rotors. CyMGs with CP rotors require less PM pieces than CyMGs with SPM rotors, which may simplify manufacturing. Each topology is optimized using a genetic algorithm with 2D finite element analysis (FEA). The simulation results demonstrate that CyMGs with CP rotors achieve lower VTD values than CyMGs with SPM rotors. However, if using a CP inner rotor eliminates the need for a PM retention sleeve and enables the use of a smaller effective air gap, CyMGs with CP rotors can achieve higher PM STs at high gear ratios than CyMGs with SPM rotors. CyMGs with CP rotors generally experience similar perpendicular magnetic forces and slightly higher eccentric magnetic forces, relative to CyMGs with SPM rotors. The optimal 2D designs are further investigated using 3D FEA, and, within this design set, the CyMGs with CP rotors experience more significant end effects than the CyMGs with SPM rotors.**

Keywords—Consequent pole, cycloidal magnetic gear, finite element analysis (FEA), gear ratio, genetic algorithm, optimization, specific torque, surface permanent magnet, torque density

I. Introduction

This paper investigates the effects of utilizing a consequent pole (CP) structure in cycloidal magnetic gears (CyMGs), as shown in Fig. 1. The CP topology is an alternative to the surface permanent magnet (SPM) topology; all of the permanent magnets (PMs) on a CP rotor are magnetized in the same direction, and ferromagnetic teeth fill the spaces between PMs. A CP CyMG is potentially more robust and can facilitate the use of a smaller air gap than an SPM CyMG because the CP configuration's PM slots can be designed to naturally retain the PMs, thus eliminating the need for a sleeve around the inner rotor to keep the PMs in place. This study focuses on optimizing and comparing the performances of CyMGs with the different rotor combinations listed in Table I and shown in Fig. 1.

Magnetic gears have been proposed as an alternative to mechanical gears for a wide range of applications from wind [1] and wave [2] energy harvesting, to electric vehicles [3], electric aviation [4], and space applications [5]. Due to their noncontact operation, magnetic gears offer potential advantages with respect to a plethora of considerations, such as inherent overload protection and isolation between shafts. Most research on magnetic gears investigates coaxial magnetic gears, especially for low gear ratio applications [1]-[4], [6]; however, cycloidal magnetic gears, such as the one shown in Fig. 1(a), have received attention for high gear ratio applications [5], [7]-[9].

A CyMG uses a non-uniform, time-varying air gap to modulate the magnetomotive force (MMF) of the PMs on each rotor. This is similar to the role of the modulators in a coaxial

TABLE I. Evaluated CyMG Rotor Configurations

Rotor Configuration	Abbreviation
SPM inner rotor and SPM outer rotor	SPM-SPM
CP inner rotor and SPM outer rotor	CP-SPM
CP inner rotor and CP outer rotor	CP-CP

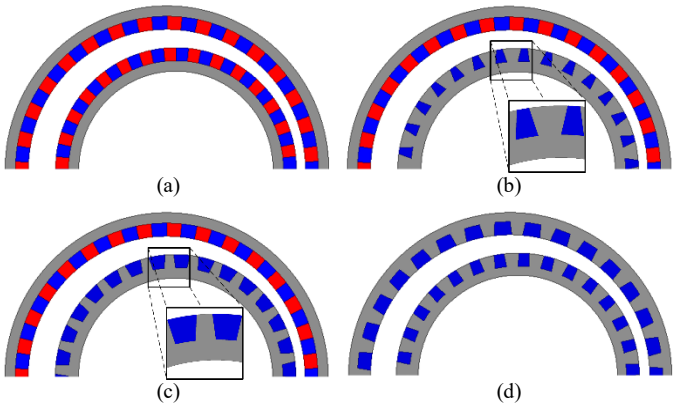

Fig. 1. Cross-sections of (a) an SPM-SPM CyMG, (b) a CP-SPM CyMG with the inner rotor teeth shaped to retain the PMs, (c) a CP-SPM CyMG with the inner rotor teeth not shaped to retain the PMs, and (d) a CP-CP CyMG.

This work was supported in part by the U.S. Army Research Laboratory and was accomplished under Cooperative Agreement Number W911NF-18-2-0289. The views and conclusions contained in this document are those of the authors and should not be interpreted as representing the official policies, either expressed or implied, of the Army Research Laboratory or the U.S. Government. The U.S. Government is authorized to reproduce and distribute reprints for Government purposes notwithstanding any copyright notation herein.

magnetic gear. CyMGs can achieve significantly higher specific torques at higher gear ratios than coaxial magnetic gears [8]. A CyMG's outer rotor has one more pole pair than its inner rotor, as indicated by

$$P_{Out} = P_{In} + 1, \tag{1}$$

where P_{In} and P_{Out} are the pole pair counts on the inner and outer rotors, respectively. If the outer rotor is fixed, P_{In} governs the gear ratio (G) of a design, as given by

$$G = \frac{\omega_{Orb}}{\omega_{Rot,In}} = -P_{In}, \tag{2}$$

where $\omega_{Rot,In}$ is the speed of the inner rotor's rotation about its own axis and ω_{Orb} is the speed of the inner rotor's orbital revolution about the axis of the outer rotor. The negative sign in (2) indicates that these motion components are in opposite directions. This motion is illustrated in Fig. 2 [8]. As described in [9], other operation modes are possible, but it is most common to fix the outer rotor and use the gear ratio given by (2).

Retaining the PMs on the inner rotor as it simultaneously orbits and rotates in a CyMG is a significant challenge. The inner rotor PMs can be retained with a sleeve, but this increases the effective air gap between the rotors, which decreases the slip torque. Using the CP topology on the inner rotor may eliminate the need for a retention sleeve if the CP teeth are shaped to retain the PMs, as shown in Fig. 1(b). Additionally, the CP topology may simplify assembly by making it easier to position the PMs by providing slots for the PMs, even if the teeth are not shaped to retain the PMs. The CP topology can further simplify assembly by reducing the piece count, as PM pieces can be replaced with teeth that are part of a single piece (likely a stack of steel laminations).

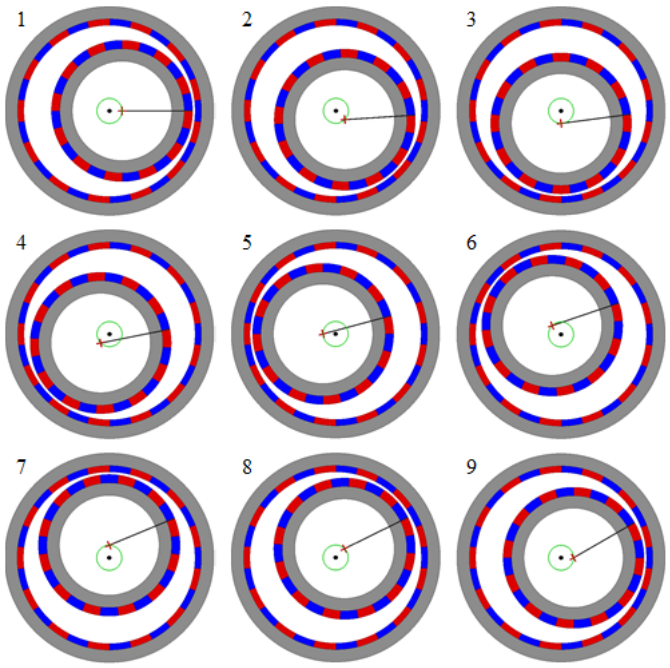

Fig. 2. Example 12:1 CyMG operation motion sequence. From each frame to the next, the inner rotor's axis (red '+') orbits the outer rotor's axis (black dot) by 45° along the green path while the inner rotor rotates about its own axis by 3.75° in the opposite direction [8].

The CP topology has been employed in motors [10]-[12], magnetically geared motors (MGMs) [13]-[14], and coaxial magnetic gears [15]. Additionally, other studies have proposed inserting PMs between the modulators in a coaxial magnetic gear to create a CP configuration on the modulator rotor to increase the torque density [16]-[19]. However, these designs replace non-magnetic material (the slots between modulators) with PMs, which is a different topology altogether. Past studies have anecdotally compared motor [12] or magnetically geared motor [14] designs using CP configurations and claimed that the CP configuration improves the torque density relative to the SPM configuration. However, another study of electric machines claims that the CP configuration is disadvantageous [10]. These conclusions are contradictory, at least in part, due to the use of anecdotal evidence based on a limited number of designs. However, utilizing the CP configuration may affect the optimal design parameters; therefore, the CP and SPM designs should be optimized individually for a fair comparison. This was done for coaxial magnetic gears with ferrite PMs in [15], which concluded that the CP topology with ferrite PMs achieved better torque densities than the SPM topology with ferrite PMs. However, the CP topology has not been evaluated for CyMGs. This paper introduces CP CyMGs and uses a genetic algorithm (GA) and parametric 2D finite element analysis (FEA) to optimize and compare the performances of CP and SPM CyMGs with NdFeB PMs across a broad range of gear ratios. Then, 3D FEA is used to evaluate the end effects of the optimal designs.

II. Design Study Methodology

The SPM-SPM, CP-SPM, and CP-CP CyMG rotor combination topologies shown in Fig. 1 were optimized to independently maximize PM specific torque (PM ST) and volumetric torque density (VTD) across gear ratios ranging from 30:1 to 80:1 using a GA with 2D FEA. A design's PM ST is its low-speed shaft slip torque divided by its PM mass, and a design's VTD is its low-speed shaft slip torque divided by its active volume. For each optimization, the GA used 100 generations with approximately 1000 individuals in each generation. For a CP inner rotor, the PM grip is defined as half of the difference obtained by subtracting the length of the chord connecting a PM's outer corners from the length of the chord connecting its inner corners. The teeth in a CP inner rotor with a positive PM grip, such as the design illustrated in Fig. 1(b), can retain the inner rotor PMs, which eliminates the need for a sleeve and may simplify the assembly. A CP inner rotor with a negative PM grip, such as the design depicted in Fig. 1(c), does not offer any inherent PM retention benefits.

For the CP-SPM and CP-CP topologies, two different inner rotor conditions were evaluated and optimized: 1) a 0.25 mm inner rotor PM grip with a 0.75 mm magnetic air gap (no PM retention sleeve present) and 2) an unconstrained inner rotor PM grip with a 1 mm magnetic air gap (including a PM retention sleeve). Table II summarizes these different scenarios. Table III lists the parameters considered in this study and their respective ranges. For CP rotors using the arbitrary grip scenario, the PMs' normalized inner and outer pitches were allowed to vary independently. The normalized PM pitch (α_{PM})

TABLE II. LEGEND FOR DIFFERENT DESIGN CONFIGURATIONS CHARACTERIZED IN FIGS. 3-11.

	SPM-SPM	CP-SPM	CP-SPM	CP-CP	CP-CP
Air Gap (mm)	1	0.75	1	0.75	1
Inner Rotor PM Grip (mm)	N/A	0.25	Any	0.25	Any

TABLE III. GA PARAMETER VALUE RANGES

Parameter	Values	Units
Inner pole pair count (P_{In})	30 – 80	
Outer radius (R_{Out})	100	mm
Inner back iron radial thickness ($T_{BI,In}$)	0, 2 – 5[a]	mm
Inner PM radial thickness ($T_{PM,In}$)	2 – 20[b]	mm
Inner rotor PM inner pitch ($\alpha_{PM,In,In}$)[e]	0.05 – 0.95[c]	
Inner rotor PM outer pitch ($\alpha_{PM,In,Out}$)[d,e]	0.05 – 0.95	
Axis offset (T_{Off})	0.5 – 10	mm
Outer PM radial thickness ($T_{PM,Out}$)	2 – 20[b]	mm
Outer rotor PM inner pitch ($\alpha_{PM,Out,In}$)[e]	0.05 – 0.95[c]	
Outer rotor PM outer pitch ($\alpha_{PM,Out,Out}$)[d,e]	0.05 – 0.95	
Outer back iron radial thickness ($T_{BI,Out}$)	0, 2 – 5[a]	mm

[a] As very thin back irons would be difficult to fabricate, only air cores (0 mm thickness) and back irons thicker than 2 mm were considered.
[b] For most optimizations; for some PM ST optimizations, the PM thickness was constrained to 2 – 10 mm because it was clear that the optimal PM thicknesses were much smaller than 10 mm.
[c] For CP rotors; SPM rotors were constrained to have normalized pitches in the range of 0.125 to 0.5.
[d] For CP rotors with arbitrary PM grip; for SPM rotors, each PM has the same inner and outer pitch.
[e] All PM pitch values are normalized pitches based on the definition given in (3).

is defined as the ratio of the PM arc length to the arc length of one pole pair, as given by

$$\alpha_{PM} = \frac{PM\ Arc\ Length}{Pole\ Pair\ Arc\ Length}. \quad (3)$$

For CP inner rotors using the fixed 0.25 mm PM grip, the normalized inner PM pitch was allowed to vary, while the normalized outer PM pitch was set to achieve the 0.25 mm PM grip. The normalized pitch of the PMs on an SPM rotor was allowed vary between 0.125 and 0.5 (half of a pole pair arc). All designs were simulated using NdFeB N52H for the PMs and M15 (29 gauge) for the back irons and CP teeth.

III. RESULTS

Figs. 3(a) and (b) show the maximum VTD and PM ST values achieved for each of the different design configuration scenarios across the range of considered gear ratios. As illustrated in Figs. 3(a) and (b), at lower gear ratios, the optimal SPM-SPM CyMGs perform better than the CP-SPM and CP-CP CyMGs in terms of both VTD and PM ST. However, at higher gear ratios, the CP-SPM and CP-CP scenarios with thinner air gaps achieve higher PM STs, as shown in Fig. 3(b). Within the considered gear ratio range the CP-SPM and CP-CP CyMGs never match the SPM-SPM CyMGs in terms of VTD, but the CP-SPM CyMGs do get very close at the very high gear ratios, as shown to the right of Fig. 3(a), and would likely surpass the SPM-SPM CyMGs in terms of VTD if even higher gear ratios were considered. However, because the CP rotor configuration replaces NdFeB PMs with soft magnetic material, it is not surprising that the CP-SPM and CP-CP topologies do not yield

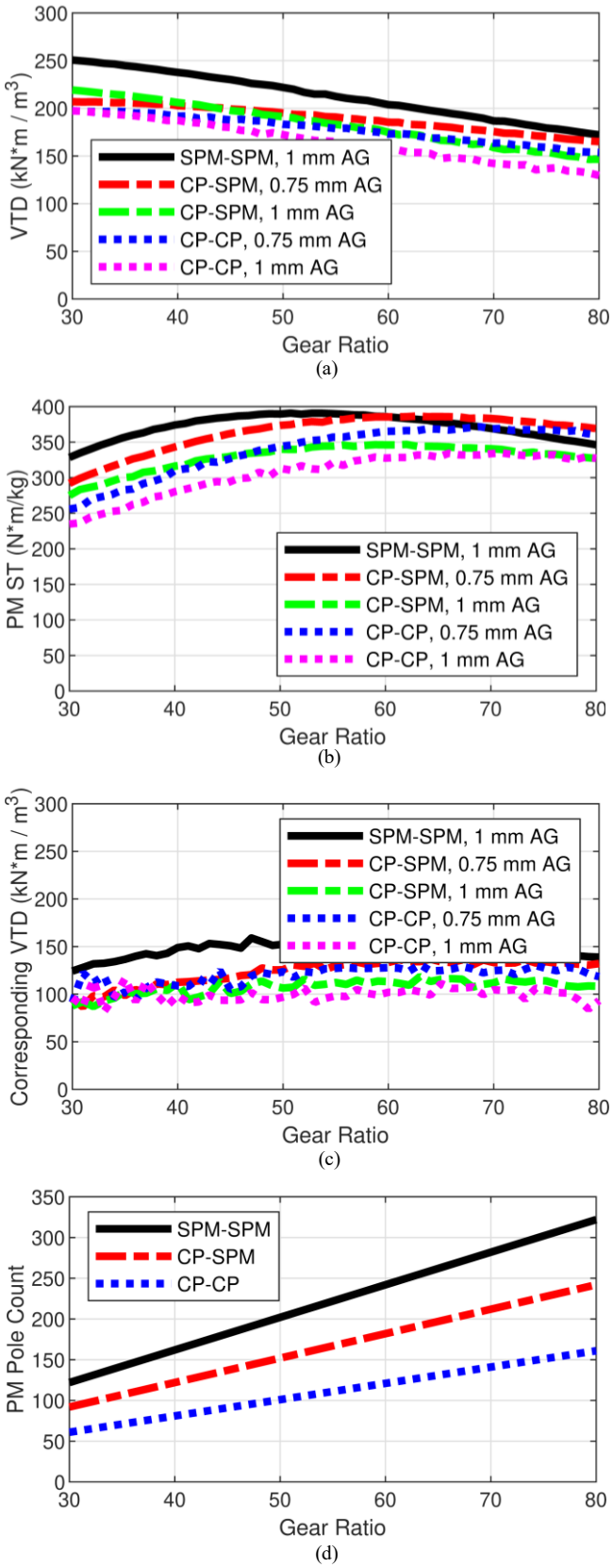

Fig. 3. The maximum (a) VTDs and (b) PM STs achieved for each GA optimization scenario across a range of gear ratios. The (c) VTDs of the designs achieving the maximum PM STs and (d) the PM pole counts required to achieve a range of gear ratios for each of the different topologies.

higher VTDs than the SPM-SPM topology. Thus, these results indicate that the CP-SPM and CP-CP topologies are more appropriate for applications where particularly large gear ratios are required or reducing the cost is more important than reducing the volume. Fig. 3(c) depicts the corresponding VTD values for the designs with the maximum PM ST values, which are shown in Fig 3(b). Relative to the SPM-SPM topology, using the CP-SPM topology to increase the PM ST at high gear ratios does result in a lower VTD, but this penalty is less than 15%.

Based on (2), a higher gear ratio requires a higher PM pole pair count, which makes the pole arcs of the PM pieces shorter and increases the tangential leakage flux. A CP rotor replaces half of the PMs on an SPM rotor with ferromagnetic teeth and, consequently, only uses half as many PM poles as the SPM rotor. Fig. 3(d) compares the number of PM poles required for each topology to achieve the various gear ratios. This demonstrates one of the main advantages of using CP rotors. Relative to the SPM-SPM topology, the CP-SPM topology requires almost 25% fewer PM poles, and the CP-CP topology only requires half as many PM poles as the SPM-SPM topology. This reduction in piece count, along with the PM insertion slots created by the CP teeth, can potentially reduce assembly costs.

In addition to reducing the piece count, replacing half of the PM poles on a rotor with ferromagnetic teeth also allows the arc lengths of the remaining PMs on a CP rotor to be increased beyond half of the pole pair arc length with a corresponding decrease in teeth arc lengths. On the other hand, it is not possible to increase the arc lengths of all of the PMs on an SPM rotor beyond half of the pole pair arc length. Fig. 4(a) shows the corresponding normalized PM pitches at the outer radius of the inner rotor for the maximum PM ST designs. The CP-SPM and CP-CP CyMGs with the maximum PM ST values favor normalized PM pitches larger than 0.5, indicating that the PMs are wider than the teeth. Consequently, the PM arc lengths of the optimal CP CyMGs are longer than those of the optimal SPM CyMGs at the same gear ratio, as shown in Fig. 4(b). The CP rotor's ability to facilitate the use of larger magnet pieces may help with manufacturing considerations, especially at high gear ratios, where the PMs can become extremely small. Note that, as illustrated in Figs. 1(b) and (c), the PM pitch can be different at the inner and outer edges of a CP CyMG's inner rotor PMs. The CP-SPM and CP-CP designs using the arbitrary PM grip scenario converge to designs with significantly negative grips, as shown in Fig. 4(c). Thus, the positive PM grip constraints are magnetically suboptimal. However, the smaller magnetic air gap resulting from the elimination of the PM retention sleeve (which is enabled by positive PM grips) allows these designs to outperform the negative PM grip designs with larger air gaps, especially at larger gear ratios. Fig. 4(d) shows the corresponding PM arc lengths at the inner radius of the outer rotor PMs. As on the inner rotor, using a CP outer rotor results in larger optimal PM arc lengths, which can simplify manufacturing, particularly at high gear ratios.

Figs. 5(a)-(e) display the cross sections of the optimal designs with maximum VTD for each topology, corresponding to the results in Fig. 3(a). Similarly, Figs. 6(a)-(e) depict the cross sections of the maximum PM ST designs, corresponding to the results in Fig. 3(b). Comparing the maximum PM ST

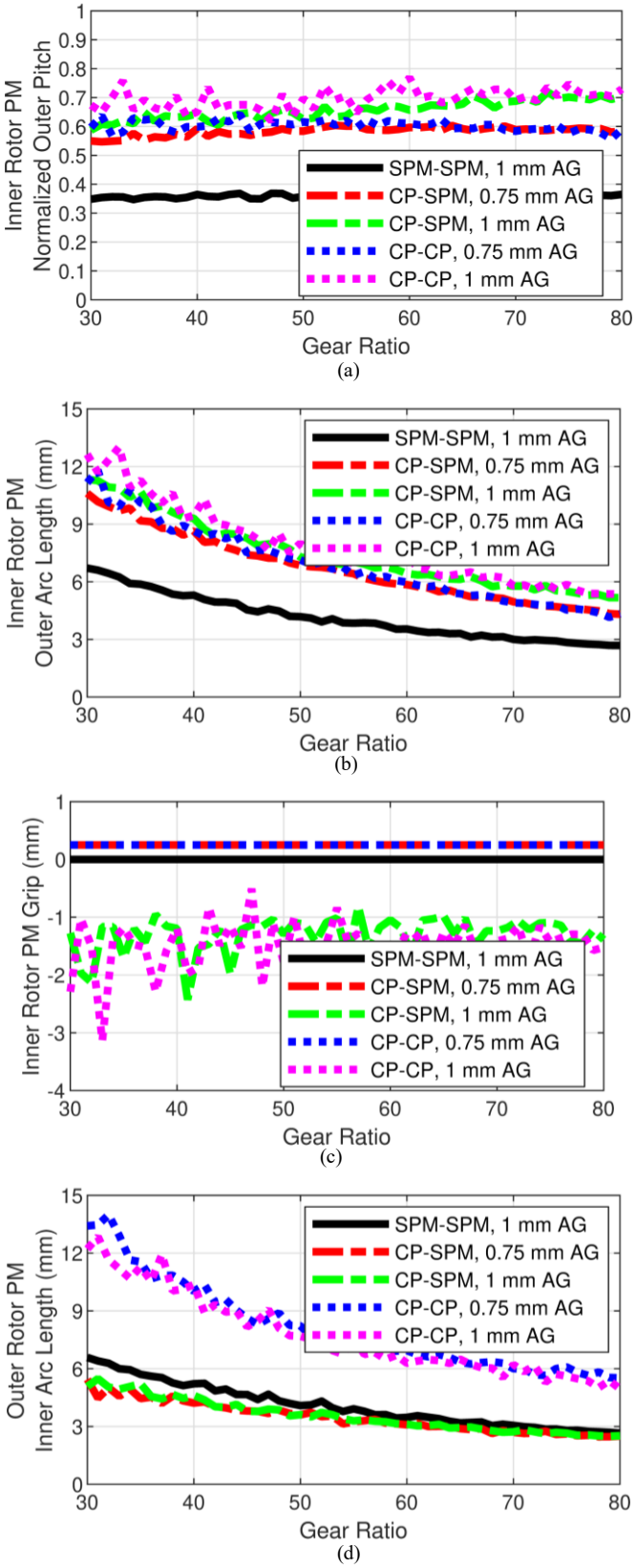

Fig. 4. The corresponding (a) inner rotor PM normalized outer pitch, (b) inner rotor PM outer are length, (c) inner rotor PM grip, and (d) outer rotor PM inner arc length for the designs with the maximum PM ST values given in Fig. 3(b).

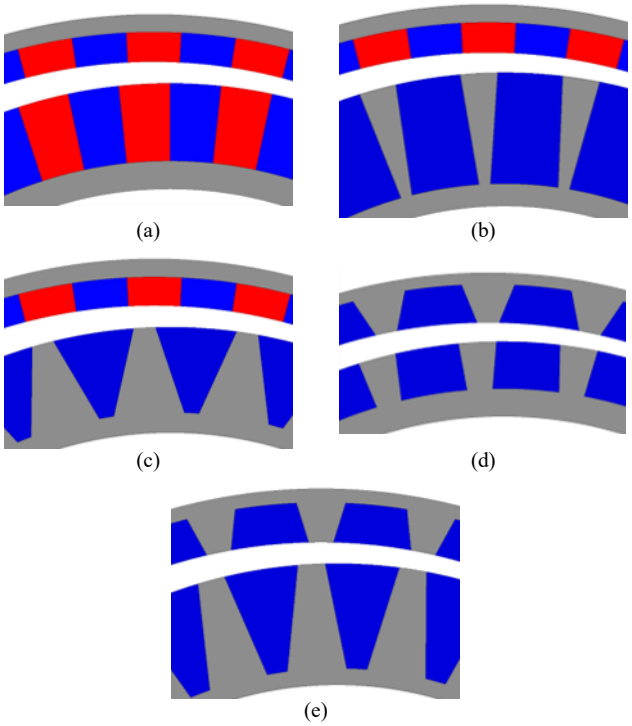

Fig. 5. Cross-sectional portions of (a) the SPM-SPM CyMG, (b) the CP-SPM CyMG with a 0.25 mm inner rotor PM grip, (c) the CP-SPM CyMG with an arbitrary inner rotor PM grip, (d) the CP-CP CyMG with a 0.25 mm inner rotor PM grip, and (e) the CP-CP CyMG with an arbitrary inner rotor PM grip that achieve the maximum VTD.

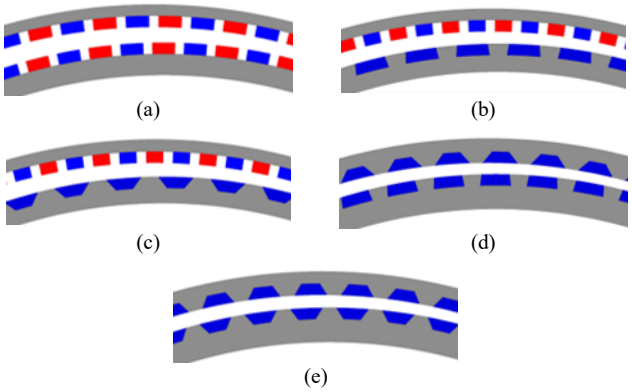

Fig. 6. Cross-sectional portions of (a) the SPM-SPM CyMG, (b) the CP-SPM CyMG with a 0.25 mm inner rotor PM grip, (c) the CP-SPM CyMG with an arbitrary inner rotor PM grip, (d) the CP-CP CyMG with a 0.25 mm inner rotor PM grip, and (e) the CP-CP CyMG with an arbitrary inner rotor PM grip that achieve the maximum PM ST.

designs reveals that the PM pieces on the CP rotors are wider than those on the SPM rotors. The ability of CP rotors to use wider PM pieces at a given gear ratio and achieve smaller air gaps result in a higher optimum gear ratio with respect to maximizing PM ST, as compared to SPM rotors. Fig. 5 demonstrates that optimization of a topology for VTD leads to designs with thicker PMs, especially on the inner rotor. Utilizing thicker PMs on the outer rotor decreases the air gap radius (assuming a fixed outer radius), which reduces its slip torque. Thus, there is a tradeoff between the increased flux density benefits of increasing the thickness of the outer rotor PMs and the deleterious consequences of the associated reduction in the air gap radius. Increasing the thickness of the PMs on the inner rotor does not reduce the air gap radius (assuming a fixed outer radius).

The magnetic forces acting on the inner rotor are also key aspects of the design [5], [20]-[22]. These forces increase the load upon the bearing between the high-speed shaft and the inner rotor [5], reducing its expected lifetime and increasing losses. As the electromagnetic losses in CyMGs are relatively small [5], [23], the friction losses tend to be the dominant source of losses [5]. Consequently, these forces can have a large impact on efficiency. Figs. 7 and 8 show the normalized torques and magnetic forces exerted on the inner rotor as a function of the

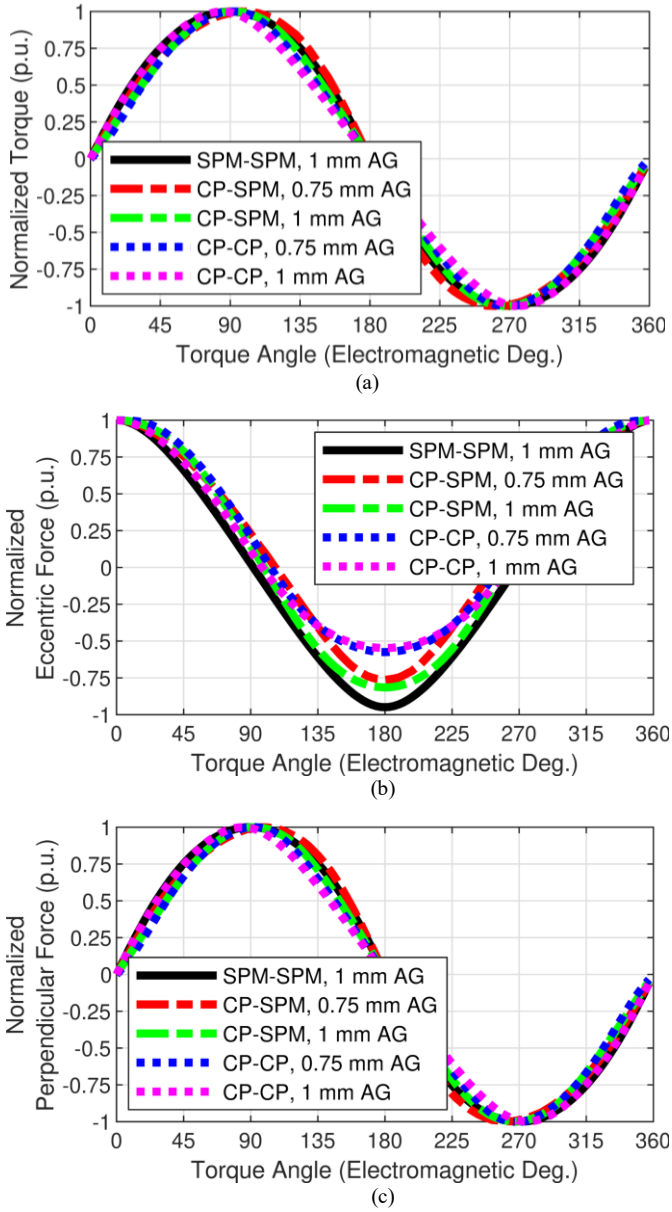

Fig. 7. The normalized magnetic (a) torque, (b) eccentric force, and (c) perpendical force exerted on the inner rotor as a function of torque angle for the CyMG designs with the highest VTDs for each topology.

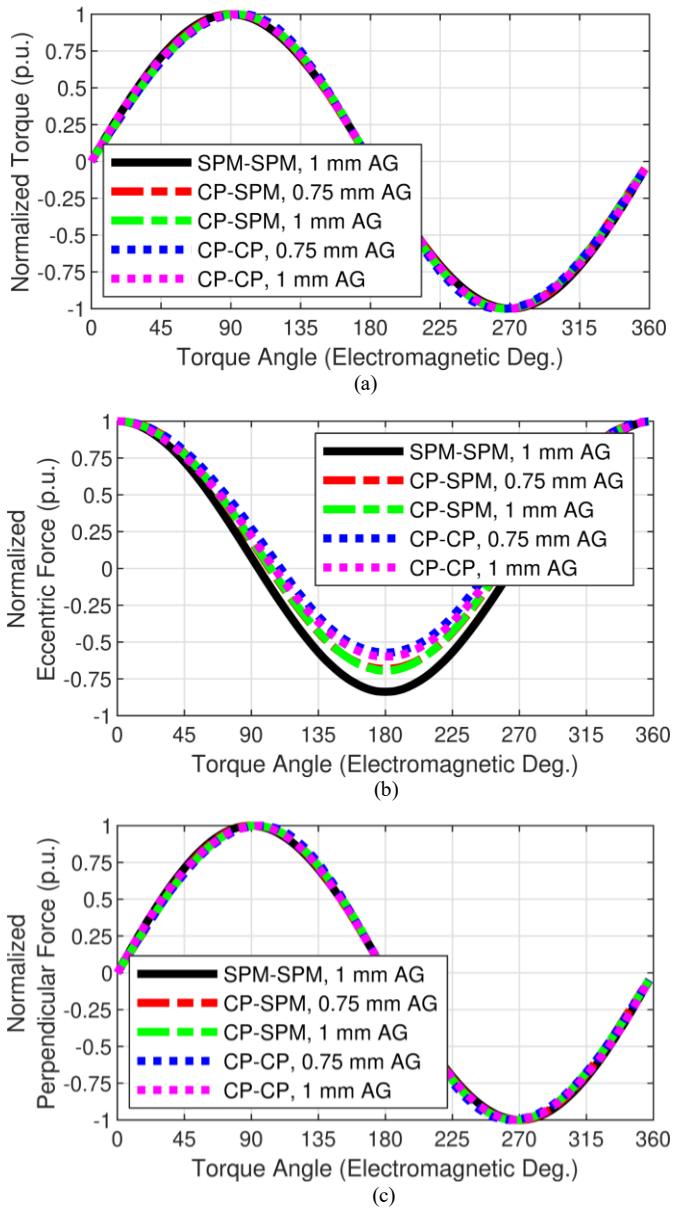

Fig. 8. The normalized magnetic a) torque, (b) eccentric force, and (c) perpendical force exerted on the inner rotor as a function of torque angle for the CyMG designs with the highest PM STs for each topology.

torque angle (the difference in the electromagnetic angles of the rotors where the air gap is smallest) for the designs with the highest VTDs and PM STs for each topology. For comparison purposes, each torque or force versus torque angle curve for a given design in Figs. 7 and 8 is normalized by its own maximum value and not by the overall maximum value in the graph.

The eccentric forces shown in Figs. 7(b) and 8(b) are the magnetic forces in the direction of the axis offset. For the CyMG shown in step 1 of Fig. 2, the eccentric force is the force on the inner rotor oriented along the x-axis. The perpendicular forces shown in Figs. 7(c) and 8(c) are the magnetic forces in the direction perpendicular to the axis offset. For the CyMG shown in step 1 of Fig. 2, the perpendicular force is the force on the inner rotor oriented along the y-axis. The torques shown in Figs. 7(a) and 8(a) are approximately sinusoidal, although the torques of the maximum VTD designs with CP rotors tend to be slightly less sinusoidal than those of the other designs. The eccentric forces are also sinusoidal with a maximum at the zero torque angle. However, the eccentric forces have a non-zero average with respect to torque angle, and the average eccentric forces of the designs with CP rotors are larger than those of the SPM-SPM designs. This means that the designs with CP rotors have a larger eccentric force at high loads. This is noteworthy because this eccentric force could be used to partially mitigate the pin reaction forces [5]. The perpendicular forces shown in Figs. 7(c) and 8(c) are responsible for generating the torques, and have a similar profile to the torques shown in Figs. 7(a) and 8(a). Figs. 9 and 10 compare the no load eccentric forces and peak load perpendicular forces for each of the maximum VTD and PM ST designs characterized in Figs. 3(a) and (b), each scaled to the stack length required to produce a 100 N·m slip torque, based on 2D FEA. For the same slip torque, both the perpendicular and eccentric forces of the optimal designs tend to decrease slightly as the gear ratio increases. The perpendicular forces at the maximum torque angle are relatively consistent across all topologies. However, the CP-CP topology has larger eccentric forces at no load than the other topologies.

Another important consideration is end effects. It is well established that end effects are often very significant for coaxial magnetic gears [24]. However, end effects can also be significant for CyMGs [8]. While the previous results are based on 2D FEA, Fig. 11 shows the significance of the end effects for

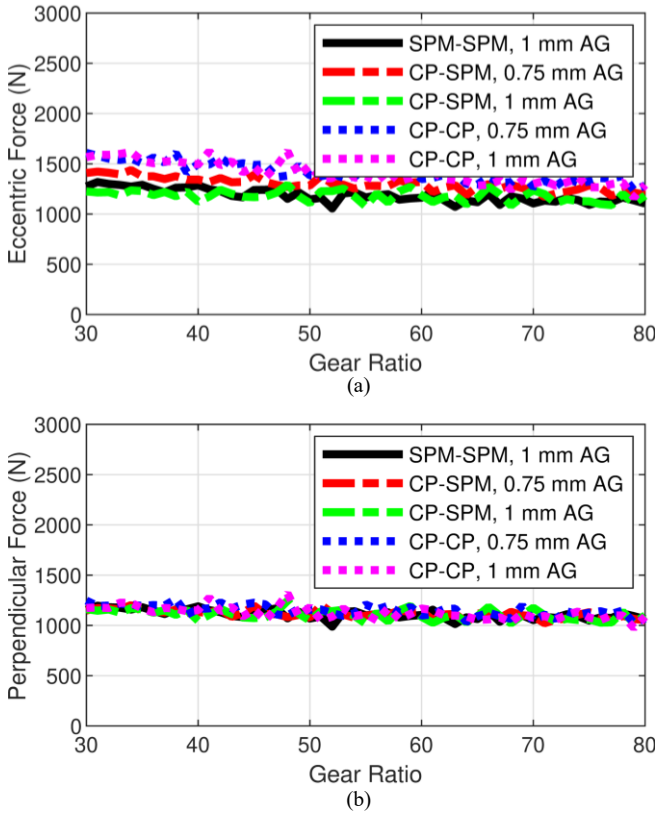

Fig. 9. Inner rotor (a) No load eccentric forces and (b) peak load perpendicular forces for the CyMG designs with the highest VTDs for each topology at each gear ratio (corresponding to the designs characterized in Fig. 3(a)).

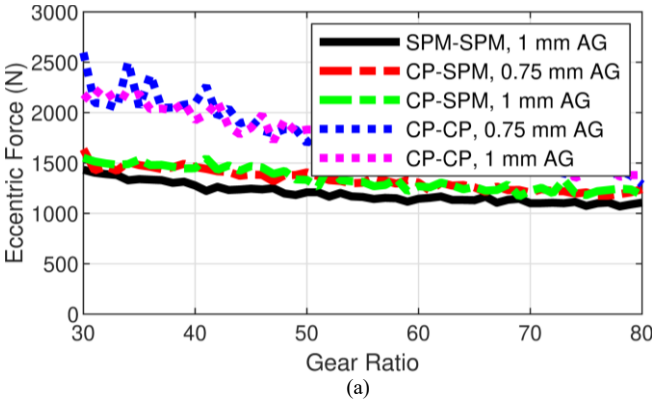

(a)

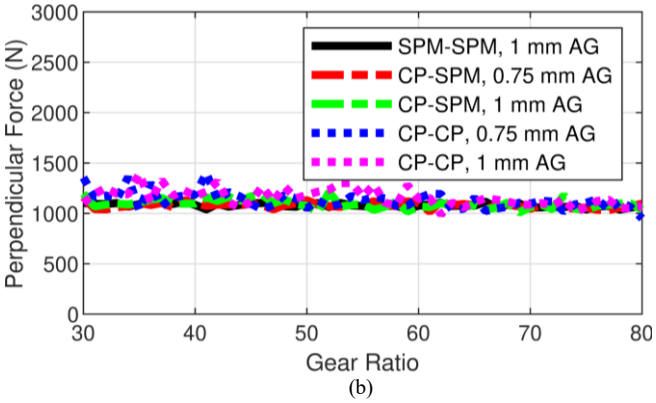

(b)

Fig. 10. Inner rotor (a) No load eccentric forces and (b) peak load perpendicular forces for the CyMG designs with the highest PM STs for each topology at each gear ratio (corresponding to the designs characterized in Fig. 3(b)).

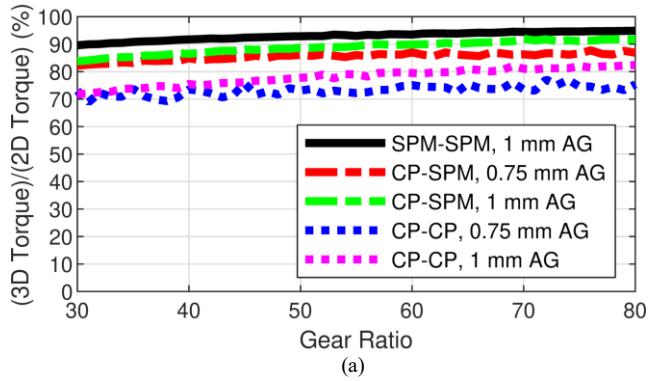

(a)

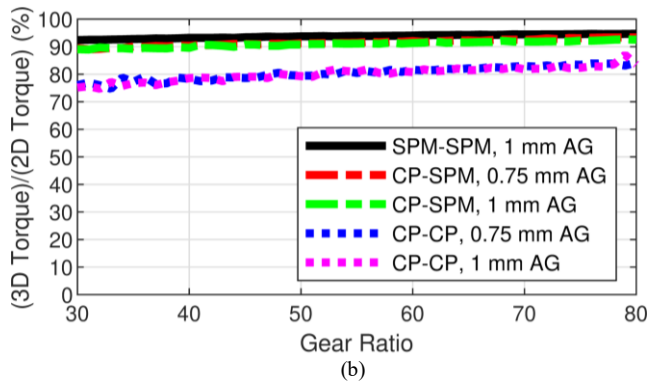

(b)

Fig. 11. Significance of 3D effects on slip torque for (a) the maximum VTD designs and (b) the maximum PM ST designs of each topology at a stack length of 25 mm.

the optimal VTD and PM ST designs depicted in Figs. 3(a) and (b) at a 25 mm stack length, based on 3D FEA. The maximum VTD designs tend to suffer more significant end effects than the maximum PM ST designs. Additionally, the CP-CP designs tend to suffer more significant end effects than the CP-SPM and SPM-SPM designs, and the SPM-SPM designs tend to experience less significant end effects than the CP-CP and CP-SPM designs.

IV. Conclusion

This study uses 2D FEA simulations to compare cycloidal magnetic gears (CyMGs) with different combinations of surface permanent magnet (SPM) rotors and consequent pole (CP) rotors, as summarized in Table I. A basic analysis of the different topologies along with a review of the simulation results supports the following general conclusions within the evaluated design space:

- CyMGs with CP rotors require less PM pieces than CyMGs with SPM rotors, which may simplify manufacturing.
- CyMGs with CP rotors provide inherent PM insertion slots, which may simplify manufacturing relative to CyMGs with SPM rotors.
- CyMGs with CP rotors achieve lower VTD values than CyMGs with SPM rotors.
- CyMGs with CP rotors can use PMs with wider arc lengths than CyMGs with SPM rotors. The use of wider PMs provides some potential practical manufacturing advantages and results in CyMGs with CP rotors exhibiting a higher optimum gear ratio for maximizing PM ST than CyMGs with SPM rotors.
- CyMGs with CP inner rotors can be designed to inherently retain the PMs, thus potentially eliminating the need for a PM retention sleeve and enabling the use of a smaller effective air gap.
- If using a CP inner rotor eliminates the need for a PM retention sleeve and enables the use of a smaller effective air gap, CyMGs with CP inner rotors can achieve higher PM STs than CyMGs with SPM inner rotors at higher gear ratios.
- Optimized CyMGs with CP rotors do not necessarily achieve higher PM STs than optimized CyMGs with SPM rotors if they use the same air gap, except possibly at gear ratios beyond the range evaluated in this study and much higher than the optimal gear ratios.
- CyMGs with CP rotors experience slightly higher eccentric magnetic forces at no load than CyMGs with SPM rotors.
- CyMGs with CP rotors experience higher eccentric magnetic forces at full load than CyMGs with SPM rotors.
- CyMGs with CP rotors and SPM rotors experience very similar perpendicular magnetic forces.

- CP-CP CyMGs optimized with 2D FEA exhibit a larger slip torque reduction when evaluated with 3D FEA due to end effects than CP-SPM and SPM-SPM CyMGs optimized with 2D FEA.

ACKNOWLEDGMENT

Portions of this research were conducted with the advanced computing resources provided by Texas A&M High Performance Research Computing. The authors would like to thank ANSYS for their support of the EMPE lab through the provision of FEA software.

REFERENCES

[1] N. Frank and H. Toliyat, "Gearing ratios of a magnetic gear for wind turbines," in *Proc. IEEE Int. Elect. Mach. Drives Conf.*, 2009, pp. 1224–1230.

[2] K. K. Uppalapati, J. Z. Bird, D. Jia, J. Garner, and A. Zhou, "Performance of a magnetic gear using ferrite magnets for low speed ocean power generation," in *Proc. IEEE Energy Convers. Congr. Expo.*, 2012, pp. 3348–3355.

[3] T. Frandsen, L. Mathe, N. Berg, R. Holm, T. Matzen, P. Rasmussen, and K. Jensen, "Motor integrated permanent magnet gear in a battery electrical vehicle," *IEEE Trans. Ind. Appl.*, vol. 51, no. 2, pp. 1516–1525, Mar.-Apr. 2015.

[4] T. F. Tallerico, Z. A. Cameron, J. J. Scheidler, and H. Hasseeb, "Outer stator magnetically-geared motors for electrified urban air mobility vehicles," in *Proc. AIAA/IEEE Elect. Aircraft Technol. Symp.*, 2020, pp. 1-25.

[5] B. Praslicka et al., "Practical analysis and design of a 50:1 cycloidal magnetic gear with balanced off-axis moments and a hgh specific torque for lunar robots," in *Proc. IEEE Int. Elect. Mach. Drives Conf.*, 2021, pp. 1-8.

[6] M. C. Gardner, M. Johnson, and H. A. Toliyat, "Analysis of high gear ratio capabilities for single-stage, series multistage, and compound differential coaxial magnetic gears," *IEEE Trans. Energy Convers.*, vol. 34, no. 2, pp. 665-672, Jun. 2019.

[7] J. Rens, K. Atallah, S. D. Calverley, and D. Howe, "A novel magnetic harmonic gear," *IEEE Trans. Ind. Appl.*, vol. 46, no. 1, pp. 206-212, Jan.-Feb. 2010.

[8] M. C. Gardner, M. Johnson, and H. A. Toliyat, "Comparison of surface permanent magnet coaxial and cycloidal radial flux magnetic gears," in *Proc. IEEE Energy Convers. Congr. and Expo.*, 2018, pp. 5005-5012.

[9] F. T. Jørgensen, T. O. Andersen, and P. O. Rasmussen, "The cycloid permanent magnetic gear," *IEEE Trans. Ind. Appl.*, vol. 44, no. 6, pp. 1659-1665, Nov.-Dec. 2008.

[10] J. A. Tapia, F. Leonardi, and T. A. Lipo, "Consequent-pole permanent-magnet machine with extended field-weakening capability," *IEEE Trans. Ind. Appl.*, vol. 39, no. 6, pp. 1704-1709, Nov.-Dec. 2003.

[11] S. Chung, J. Kim, Y. Chun, B. Woo, and D. Hong, "Fractional slot concentrated winding PMSM with consequent pole rotor for a low-speed direct drive: reduction of rare earth permanent magnet," *IEEE Trans. Energy Conv.*, vol. 30, no. 1, pp. 103-109, Mar. 2015.

[12] Y. Ueda, H. Takahashi, T. Akiba, and M. Yoshida, "Fundamental Design of a Consequent-Pole Transverse-Flux Motor for Direct-Drive Systems," *IEEE Trans. Magn.*, vol. 49, no. 7, pp. 4096-4099, Jul. 2013.

[13] H. Huang, L. Jing, R. Qu, and D. Li, "The demagnetizing protection of Halbach consequent pole in a magnetic-geared machine," in *Proc. Int. Conf. Elect. Mach. and Sys.*, 2018, pp. 365-370.

[14] H. Huang, D. Li, W. Kong, and R. Qu, "Torque performance of pseudo direct-drive machine with Halbach consequent pole," in *Proc. IEEE Energy Convers. Congr. Expo.*, 2018, pp. 3286-3293.

[15] J. Shen, H. Li, H. Hao, and M. Jin, "A coaxial magnetic gear with consequent-pole rotors," *IEEE Trans. Energy Conv.*, vol. 32, no. 1, pp. 267-275, Mar. 2017.

[16] H. Y. Wong, J. Z. Bird, S. Modaresahmadi, and W. Williams, "Comparative analysis of a coaxial magnetic gear with a flux concentration rotor and consequent pole rotor typology," *IEEE Trans. Magn.*, vol. 54, no. 11, pp. 1-5, Nov. 2018.

[17] S. Peng, W. N. Fu, and S. L. Ho, "A novel high torque-density triple-permanent-magnet-excited magnetic gear," *IEEE Trans. Magn.*, vol. 50, no. 11, pp. 1-4, Nov. 2014.

[18] W. N. Fu and L. Li, "Optimal design of magnetic gears with a general pattern of permanent magnet arrangement," *IEEE Trans. Appl. Supercond.*, vol. 26, no. 7, pp. 1-5, Oct. 2016.

[19] Y. Chen, W. N. Fu, and W. Li, "Performance analysis of a novel triple-permanent-magnet- excited magnetic gear and its design method," *IEEE Trans. Magn.*, vol. 52, no. 7, pp. 1-4, Jul. 2016.

[20] H. Huang, J. Z. Bird, A. L. Vera, and R. Qu, "An axial cycloidal magnetic gear that minimizes the unbalanced radial force," *IEEE Trans. Magn.*, vol. 56, no. 7, pp. 1-10, Jul. 2020.

[21] K. Davey, L. McDonald, and T. Hutson, "Axial flux cycloidal magnetic gears," *IEEE Trans. Magn.*, vol. 50, no. 4, pp. 1-7, Apr. 2014.

[22] K. Davey, T. Hutson, L. McDonald, and G. Hutson, "The design and construction of cycloidal magnetic gears," in *Proc. IEEE Int. Elect. Mach. Drives Conf.*, 2017, pp. 1-6.

[23] K. Li, J. Bird, J. Kadel, and W. Williams, "A flux-focusing cycloidal magnetic gearbox," *IEEE Trans. Magn.*, vol. 51, no. 11, pp. 1-4, Nov. 2015.

[24] S. Gerber and R-J. Wang, "Analysis of the end-effects in magnetic gears and magnetically geared machines," in *Proc. Int. Conf. Elect. Mach.*, 2014, pp. 396-402.